Electron-phonon coupling across the superconductor-insulator transition

T. Levinson,* A. Doron, F. Gorniaczyk, and D. Shahar
Department of Condensed Matter Physics, The Weizmann Institute of Science, Rehovot 76100, Israel

(Received 3 September 2019; revised manuscript received 30 October 2019; published 13 November 2019)

We measured current-voltage characteristics on both sides of the magnetic-field-driven superconductor-insulator transition. On both sides, these show strong nonlinearities leading to a conduction branch that is independent of phonon temperature. We show that a picture of electron overheating can quantitatively explain our data over the entire magnetic field range. We find that electron-phonon coupling strength remains roughly constant throughout the insulating state and across the superconductor-insulator transition, dropping dramatically as the magnetic field approaches zero. Our findings shed light on the origin of the highly debated saturation of resistance at low temperature, which has been interpreted by some as evidence for a new anomalous metallic phase and by others as a result of electrons failing to cool down. At the heart of this treatment lies the assumption that resistance is a function of electron temperature and not the phononic one. The applicability of this framework implies that the conduction mechanism, present in the superconductor and throughout the insulating phase, does not rely on a phonon bath.

DOI: 10.1103/PhysRevB.100.184508

I. INTRODUCTION

Highly disordered superconductors can undergo a transition to an insulating state. This superconductor-to-insulator transition (SIT) can be driven by several parameters such as disorder strength, thickness, or magnetic field strength (B) [1–4]. Subjecting such systems to an external B leads to a rich set of transport phenomena. A sample that is superconducting (SC) at $B = 0$ can, in the presence of a B, have resistance (R) that saturates at temperature (T) approaching zero. As B is further increased above a critical field (B_c) the system can enter an insulating state in which the magnetoresistance (MR) has a typical peak shape [5–7]. This B-driven insulator is comprised of Cooper pairs, as was shown by various experiments [5,8–13] and reflected in several different theoretical approaches [4,14–17]. The MR peak is considered by some as a crossover between the aforementioned Cooper-pair insulator and a fermionic one [5,18].

The saturation of $R(T \to 0) \equiv R_{\rm sat}$ in the vicinity of the SIT is a common observation and has been reported for the thickness-driven [1], B-driven [19], and carrier-concentration-driven transition [20]. Considering the most extensively studied case, the saturation in vicinity of the B-driven SIT, the experimental findings are as follows: $R_{\rm sat}$ can be orders of magnitude lower than the Drude R and is strongly dependent on B [19,21]. The range of B's at which this saturating regime is found can vary greatly [22]. There has been a longstanding theoretical effort to explain these results in terms of a metallic (finite-R) ground state, which has recently seen a surge of interest, summarized in a recent review paper [21]. The saturating R can also be explained by electronic heating without a need to invoke a novel ground state. This is because the systems in question are characterized by $R = R_0 \exp(-\Delta(B)/T)$ [19,23], which goes to 0 only at $T = 0$, and thus any saturation in effective T would result in a saturating R. This point was argued by the authors of Ref. [22], who showed that the observed $R_{\rm sat}$ was effected by filtration of the leads to the sample and was therefore sensitive to the level of external noise. One of the central arguments against this electronic-heating scenario was presented in Refs. [19,23], where the authors have measured R vs T and by fitting the high-T data, where able to infer the effective saturation T ($T_{\rm sat}$) required in order to explain $R_{\rm sat}$ in terms of electronic heating. They showed that $T_{\rm sat}$ has a strong dependence on B and that it increases as B is decreased, while $R_{\rm sat}$ showed the opposite trend. In order to explain this finding, the relevant cooling power would have to be a function of B, which decreases sharply as B is reduced.

In the insulating side of the B-driven SIT, the study of current-voltage characteristics (IV) revealed large nonlinearities and discontinuities [24,25], which were later shown [26,27] to be in quantitative agreement with an electronic overheating model formulated in Ref. [28]. In this model, which is based on a steady-state, heat-balance (HB) approach, the applied Joule-heating power is transferred from the charge carriers into the phonon bath via an electron-phonon coupling characterized by two parameters, Γ and β. The resulting equation for $T_{\rm el}$ as a function of applied V is

$$\frac{V^2}{R(T_{\rm el}(V))} = \Gamma\Omega\left(T_{\rm el}^{\beta} - T_{\rm ph}^{\beta}\right), \tag{1}$$

where Ω is the sample volume and $T_{\rm ph}$ is the phonon T in the sample. Using the general form of R in insulators $R = R_0 \exp[(T_0/T)^{\gamma}]$ we obtain

$$\frac{V^2}{R_0}\exp[-(T_0/T_{\rm el})^{\gamma}] = \Gamma\Omega\left(T_{\rm el}^{\beta} - T_{\rm ph}^{\beta}\right),$$

which can be solved numerically, reproducing the measured strong nonlinearities and discontinuities that appear below a certain T [29].

*Corresponding author: levinsontal@gmail.com

TABLE I. $\boldsymbol{\beta_0}$ and $\boldsymbol{\alpha}$ of the samples studied in this work.

Sample name	B_c [T]	β_0	α	Sample thickness [nm]
TL40a	2.1	4.75	0.7	28
TL49a	7.8	4.5	1.8	60
TL51e	2.0	4.7	1.0	41

The purpose of this article is to demonstrate that this approach can be used to explain the IV's measured throughout our magnetic field range, including the entire insulating regime as well as the SC phase down to $B = 0$.

II. RESULTS

We focused on three amorphous indium-oxide (a:InO) thin-film samples of different thicknesses, with varying levels of disorder, reflected in the values of their respective B_c's. The thicknesses and B_c's of the samples are presented in Table I, and further details can be found in the Supplemental Material [30]. We measured the IV's and low-bias R vs T curves of the samples at various B's, spanning both sides of the SIT. The measured/imposed quantity T refers to the temperature of our cryostat. For the range of electrical power applied in this work, $T \approx T_{\rm ph}$ [31], based on the well-studied Kapitza resistance between our Si substrate and the dilute ^{3}He-^{4}He coolant, and experimentally verified in our cryostat (see Supplemental Material for more details [30]). In the SC state we conducted four-terminal measurements by imposing I, and in the insulator we conducted two-terminal measurements by imposing V. Details of the measurement procedure are available in the Supplemental Material [30].

A comparison between three sets of IV's is shown in Fig. 1. IV's measured in the B-driven insulating state, as shown in previous works [26,29], are highly nonlinear. They become discontinuous below a certain T and show a T-dependent hysteresis. One of the most striking features is that the IV's measured at different T's merge at high V's, resulting in a $T_{\rm ph}$-independent conduction branch. The second set of IV's [Fig. 1(b)] was measured in a SC sample of lower disorder strength that did not undergo a B-driven SIT. These IV's share several features: strong nonlinearities, discontinuities, hysteresis, and merging high-bias branches, but with the roles of I and V exchanged. The third set of IV's [Fig. 1(c)] was measured in a sample with disorder strength close to that of the first one, in the SC state at $B < B_c$. In this case, the IV's do not show discontinuities or pronounced hysteresis but, similar to the previous two cases, the IV's are highly nonlinear and merge at high bias. Both the differential R ($\frac{dV}{dI}$) and the Ohmic one ($\frac{V}{I} \equiv R_{\rm ohm}$) are increasing functions of I and do not jump directly to the normal state R.

Due to the apparent similarities between the IV's in the SC state and those in the insulating state, we wish to analyze the IV's in the SC state in terms of electronic heating. In this work our focus is aimed at samples that undergo a B-driven SIT. In a separate work, Doron *et al.* [32] have studied lower disorder samples, that do not undergo SIT, and have shown that electronic heating can quantitatively predict the observed critical currents. We follow their approach and extend the HB treatment from the insulator to the SC state, in which we impose I rather than V, by rewriting Eq. (1) in the form $I^2R(T_{\rm el}(I)) = \Gamma\Omega(T_{\rm el}^{\beta} - T_{\rm ph}^{\beta})$. In the SC the R is typically activated [12], i.e., $R = R_0 \exp(-T_0/T)$, and thus the heat balance equation in the SC takes the form

$$I^2 R_0 \exp(-T_0/T_{\rm el}) = \Gamma\Omega\left(T_{\rm el}^{\beta} - T_{\rm ph}^{\beta}\right),$$

which is similar to the insulator, with $\gamma = 1$. Since the HB equation in the case of the SC is of the same functional form as in the insulator (with the substitution $I \leftrightarrow V$), it is obvious that electronic heating can lead to IV's that are similar to those in the insulator (again, with the substitution $I \leftrightarrow V$).

In order to show that the HB picture quantitatively describes our data obtained from the SC as well as the insulator, we use the low-bias R vs T data as a method of self-thermometry. In the limit of zero bias, $T_{\rm el} = T_{\rm ph} = T$; thus R vs T measured at low enough bias is a measure of

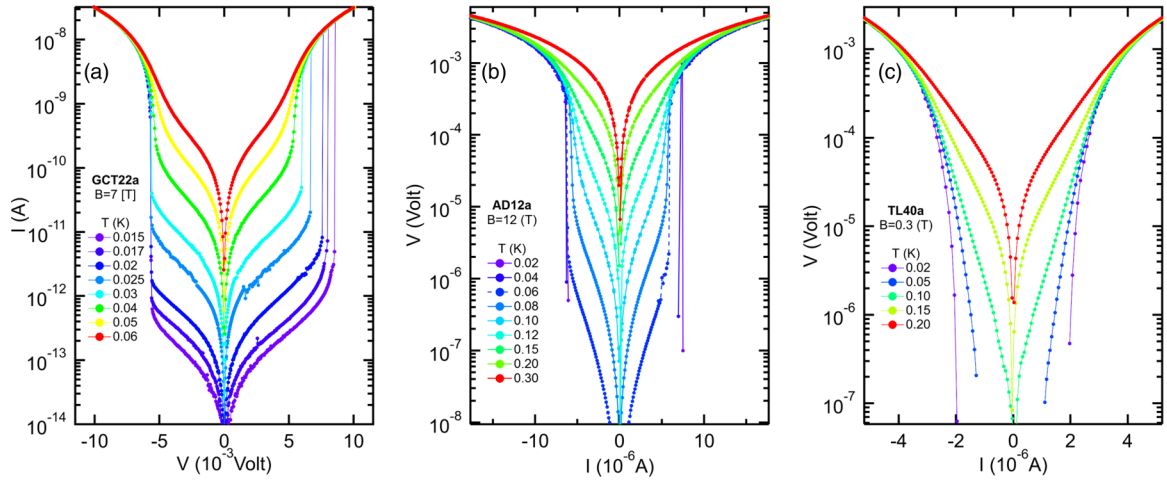

FIG. 1. Comparison of IV's between the insulating state and the SC one. (a) I vs V of sample GCT22a at $B = 7$ T, at which the sample is insulating. I is presented in absolute value, on a log scale. (b) V vs I of sample AD12a, a lower-disorder sample that did not undergo a B-driven SIT, at $B = 12$ T. V is presented in absolute value, on a log scale. (c) V vs I of sample TL40a at $B = 0.3$ T at which the sample is on the SC side of the B-driven SIT. V is presented in absolute value on a log scale. In all plots the color scales correspond to the values of T (see legends).

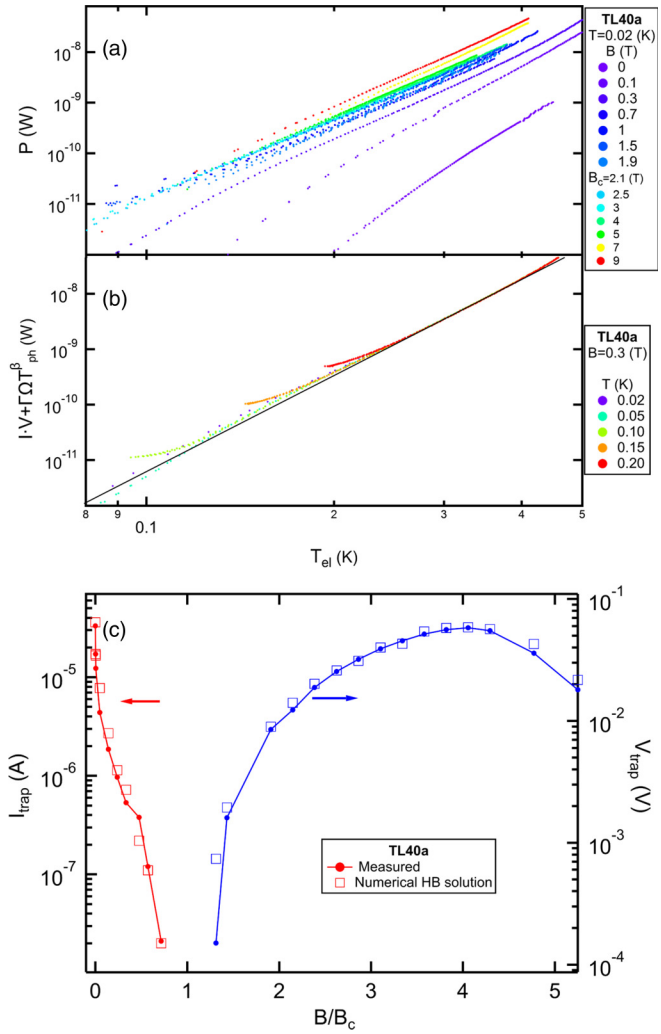

FIG. 2. Heat-balance analysis. (a) P vs inferred $T_{\rm el}$ of sample TL40a at $T = 0.02$ K for a range of $B's$ (see legend) spanning both sides of the SIT ($B_c = 2.1$ T). The data is presented in a log-log scale. (b) $P + \Gamma\Omega T_{\rm ph}^{\beta}$ vs inferred $T_{\rm el}$ of sample TL40a at $B = 0.3$ T, at which the sample is in the SC state. The color scale corresponds to different T's (see legend). The data is presented in a log-log scale. Subfigures (a) and (b) share a common x axis. (c) $I_{\rm trap}$ vs B/B_c plotted on a log-lin scale on the bottom and left axes, and $V_{\rm trap}$ vs B/B_c plotted on a log-lin scale on the bottom and right axes. Measured values are marked as circles and values acquired by graphical solution of the HB equation as squares.

$R(T_{\rm el})$. For each B in which we measured R vs T, we verified that the I or V imposed was within the linear regime of the IV. Starting from the raw IV we first calculate $R_{\rm ohm}$ and then map a $T_{\rm el}$ to each data point by using the aforementioned R vs T data [33]. In addition, we calculate the Joule-heating power $P = IV$ for each data point, ending with P vs $T_{\rm el}$ out of each IV. Several P vs $T_{\rm el}$ data sets, differing by the B at which they were measured, are plotted in Fig. 2(a). In the B range of 0.7–9 T, the data show a trend of growing P at constant $T_{\rm el}$ as B increases, which corresponds to enhancement in the electron-phonon coupling strength. The change over this entire B range is small with respect to the change that happens in the B range of 0–0.7 T, where at $T_{\rm el} = 0.2$ K, P increases by a factor of ∼100. Noticeably, no qualitative change happens at B_c (= 2.1 T). The asymptotic $[(\frac{T_{\rm el}}{T_{\rm ph}})^{\beta} \gg 1]$ power-law behavior is manifest as a straight line in the logarithmic plot. We fit this part of the data to the form $P = \Gamma\Omega(T_{\rm el}^{\beta})$ in order to obtain $\Gamma(B)$, $\beta(B)$. In Fig. 2(b) we have plotted $P + \Gamma\Omega(T_{\rm ph}^{\beta})$ for $B = 0.3$ T. With the exception of the lowest biases at each T, where the relative error is largest [34], the data collapse onto the fit. This signifies that the HB picture is consistent with the IV in the SC side, i.e., for a given B, the entire spread of $I(V, T_{\rm ph})$ data is explained by a single Γ, β. A similar analysis is presented in the Supplemental Material for other samples and other B's [30]. For the case of the insulator, this has already been shown in Ref. [26].

Besides matching the observed IV's in the sense that each point in the IV is characterized by a P and $T_{\rm el}$ that follow Eq. (1), the HB picture also describes the I and V scale at which the discontinuities or strong nonlinearities appear. We can quantify this by the I (for $B < B_c$) or V (for $B > B_c$) at which the sample jumps from the high-bias conduction branch to the low-bias one, referred to as $I_{\rm trap}$ and $V_{\rm trap}$, respectively [35]. For the B's in which the IV's are continuous, $I_{\rm trap}$ and $V_{\rm trap}$ are not well defined, but we can make a rough estimate. Based on the R vs T data and on Γ, β it is possible to numerically solve the HB equation and obtain $I_{\rm trap}$ or $V_{\rm trap}$ (more details available in the Supplemental Material [30]). Numerical solutions for $I_{\rm trap}$ and $V_{\rm trap}$ alongside the measured values are shown in Fig. 2 to be in agreement. Both $I_{\rm trap}$ and $V_{\rm trap}$ change by orders of magnitude as a function of B in the vicinity of B_c. According to the HB description, the scale of $I_{\rm trap}$ and $V_{\rm trap}$ emerges from the activation-energy scale that vanishes at the SIT [28,36], and no additional theory is necessary in order to explain this sharp behavior near B_c.

Having shown that the HB picture can quantitatively explain the IV's in both the SC and in the insulator, we use these IV's to study the electron-phonon coupling strength. In Fig. 3 we have plotted β vs $\frac{B}{B_c}$ of the three samples at the heart of this work. In the insulator, we find that β scatters within the range (5.0,5.8) and transitions smoothly across B_c into the SC. In contrast, as we approach $B = 0$, β increases significantly, showing a roughly logarithmic B dependence of the form $\beta = \beta_0 - \alpha \ln(\frac{B}{B_c})$, merging with its high-$B$ value at $B \sim B_c$ [see Fig. 3(a)]. β_0 and α best fitting each sample are presented in Table I. We would like to point out that the coupling strength found in the insulator and in the SC near B_c is (at $T \approx 0.5$ K) of the same order of magnitude as previously reported for insulating NbSi thin films [37], doped Si-on-insulator thin films [38], and metallic thin films of Au and Bi [39]. It is the coupling at low B values in the SC that is weak rather than the coupling in the insulator being particularly strong.

Our measurements of the electron-phonon coupling strength can be used in order to address the following question: Can electronic heating offer an explanation to $R_{\rm sat}$? Using the β, Γ obtained from our fits it is possible to estimate the effect of electron heating caused by external noise on $R_{\rm sat}$. We shall consider the most simplistic case, treating the effect of external noise as if a constant P ($P_{\rm ex}$) is applied to the electronic system and calculate the expected $T_{\rm sat}$. By plugging $P_{\rm ex}$ in the left-hand side of Eq. (1) and rearranging it, we derive $T_{\rm sat}(B) = (\frac{P_{\rm ex}}{\Gamma(B)\Omega})^{1/\beta(B)}$. We have treated the case of

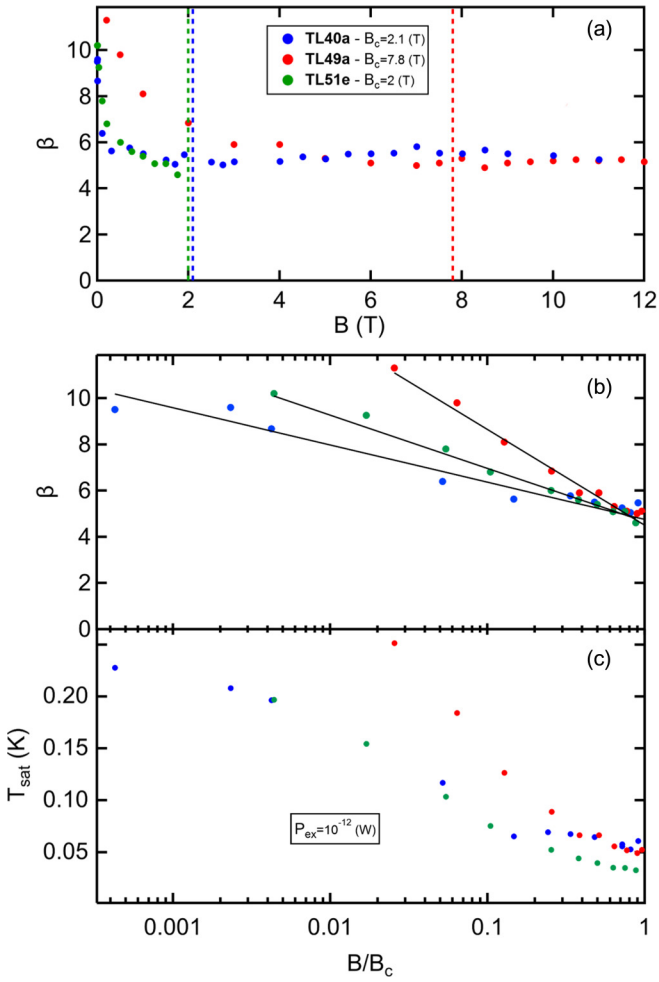

FIG. 3. Electron-phonon coupling strength and resulting saturation T's. (a) β vs B plotted on a linear scale. The sample names and corresponding B_c's are specified in the legend. The vertical dashed lines signify B_c of each sample. (b) The same data plotted on a lin-log plot. The data from the insulator is omitted from this plot. The black lines are fits to the form $\beta = \beta_0 - \alpha \ln(B/B_c)$. (c) Expected saturation T in the presence of external noise, treated as a constant $P_{ex} = 10^{-12}$ W, plotted on a linear scale vs B/B_c on a logarithmic scale. Subfigures (b) and (c) share a common x axis.

$P_{ex} = 10^{-12}$ W. This is the power that we estimate is applied on the sample placed in our cryostat due to external noise when our lines are filtered using the 200-kHz *RC* filters that were used below B_c in this work. This estimate is based on Ref. [22], in which the measurements were conducted in the same cryostat, using the same filters. T_{sat} vs B is presented in Fig. 3. We find that a logarithmic dependence of the form $T_{sat} \sim \log(1/B)$ roughly describes the predicted saturation, in qualitative agreement with the results published in Ref. [22] that show this for a wide range of systems [19,23,40].

III. CONCLUSIONS AND OUTLOOK

We have found that overheated electrons can describe the nonequilibrium transport properties of a:InO thin films on both sides of the B-driven SIT. The electron-phonon coupling strength is roughly constant throughout the insulator and across B_c. At low B's we find a significant increase in β, which corresponds to a much weaker coupling at low T's. The physical implications of the data are as follows: In the insulator, the conjecture that R is a function of T_{el}, i.e., the conduction mechanism can be fueled by an electron bath and is not reliant on a phonon bath, is contradictory to the standard picture of conduction in insulators. This was pointed out in previous work [28,37]. The HB picture was previously shown to describe the IV's of the insulating state at a B of 11 T [26]. This B is well above the MR peak where, as mentioned earlier, the conduction may be associated with fermionic quasiparticles rather than Cooper pairs. We now learn that the same heating picture takes place below the peak, where it has been established that current is carried by Cooper pairs, stressing the fact that phonon-independent conduction is present in such Cooper-pair insulators as well as in conventional ones. In the SC, at low B's we find that $\beta \sim \ln(1/B)$, reaching values of β as high as 11.3. If heating is behind the observed IV's at these B's, this dramatic weakening of the electron-phonon coupling at low B's, and subsequently much weaker cooling power, points to electron heating as the source of R_{sat}. Under the assumption that external noise acts as a constant P, electron overheating can reproduce the finding that $T_{sat} \sim \ln(1/B)$, such as observed in various experimental systems. An electron-phonon coupling characterized by a power law with β as high as 11 seems quite unreasonable. It may be that the increase in β is a result of a crossover from the power-law coupling that we have discussed to an exponential one. On the other hand, it might mean that at the lowest B's, the observed IV's are not solely a result of heating. In this case, an explanation is required for the power-law form displayed by P vs T_{el}, as well as for the T_{ph}-independent branch of the IV's.

Further study is called for at low B's in which a direct measurement of T_{el} should help shed light on the nonequilibrium behavior and may serve to settle arguments about R_{sat}. For the three samples studied in this work, the sample thickness is roughly proportional to α. A study of more samples is required in order to draw conclusions on the dependence of α on thickness and disorder strength.

ACKNOWLEDGMENTS

This research was supported by The Israel Science Foundation (ISF Grant No. 556/17) and the United States – Israel Binational Science Foundation (BSF Grant No. 2012210) and the Leona M. and Harry B. Helmsley Charitable Trust.

[1] H. M. Jaeger, D. B. Haviland, B. G. Orr, and A. M. Goldman, Phys. Rev. B **40**, 182 (1989).
[2] A. F. Hebard and M. A. Paalanen, Phys. Rev. Lett. **65**, 927 (1990).
[3] A. M. Goldman and N. Markovic, Phys. Today **51**, 39 (1998).
[4] V. F. Gantmakher and V. T. Dolgopolov, Phys. Usp. **53**, 1 (2010).

[5] M. A. Paalanen, A. F. Hebard, and R. R. Ruel, Phys. Rev. Lett. **69**, 1604 (1992).

[6] A. Doron, I. Tamir, T. Levinson, F. Gorniaczyk, and D. Shahar, Phys. Rev. B **98**, 184515 (2018).

[7] G. Sambandamurthy, L. W. Engel, A. Johansson, and D. Shahar, Phys. Rev. Lett. **92**, 107005 (2004).

[8] M. Stewart, A. Yin, J. Xu, and J. M. Valles, Science **318**, 1273 (2007).

[9] B. Sacépé, J. Seidemann, M. Ovadia, I. Tamir, D. Shahar, C. Chapelier, C. Strunk, and B. A. Piot, Phys. Rev. B **91**, 220508(R) (2015).

[10] B. Sacépé, T. Dubouchet, C. Chapelier, M. Sanque, M. Ovadia, D. Shahar, M. Feigel'man, and L. Ioffe, Nat. Phys. **7**, 239 (2011).

[11] D. Sherman, G. Kopnov, D. Shahar, and A. Frydman, Phys. Rev. Lett. **108**, 177006 (2012).

[12] G. Sambandamurthy, A. Johansson, E. Peled, D. Shahar, P. G. Björnsson, and K. A. Moler, Europhys. Lett. **75**, 611 (2006).

[13] M. Ovadia, D. Kalok, B. Sacépé, and D. Shahar, Nat. Phys **9**, 415 (2013).

[14] K. B. Efetov, Sov. Phys.-JETP **51**, 1015 (1980).

[15] M. P. A. Fisher, Phys. Rev. Lett. **65**, 923 (1990).

[16] V. M. Galitski, G. Refael, M. P. A. Fisher, and T. Senthil, Phys. Rev. Lett. **95**, 077002 (2005).

[17] Y. Dubi, Y. Meir, and Y. Avishai, Phys. Rev. B **73**, 054509 (2006).

[18] M. Steiner and A. Kapitulnik, Phys. C (Amsterdam, Neth.) **422**, 16 (2005).

[19] D. Ephron, A. Yazdani, A. Kapitulnik, and M. R. Beasley, Phys. Rev. Lett. **76**, 1529 (1996).

[20] J. Garcia-Barriocanal, A. Kobrinskii, X. Leng, J. Kinney, B. Yang, S. Snyder, and A. M. Goldman, Phys. Rev. B **87**, 024509 (2013).

[21] A. Kapitulnik, S. A. Kivelson, and B. Spivak, Rev. Mod. Phys. **91**, 011002 (2019).

[22] I. Tamir, A. Benyamini, E. Telford, F. Gorniaczyk, A. Doron, T. Levinson, D. Wang, F. Gay, B. Sacépé, J. Hone *et al.*, Sci. Adv. **5**, eaau3826 (2019).

[23] Y. Qin, C. L. Vicente, and J. Yoon, Phys. Rev. B **73**, 100505(R) (2006).

[24] G. Sambandamurthy, L. W. Engel, A. Johansson, E. Peled, and D. Shahar, Phys. Rev. Lett. **94**, 017003 (2005).

[25] T. I. Baturina, A. Y. Mironov, V. M. Vinokur, M. R. Baklanov, and C. Strunk, Phys. Rev. Lett. **99**, 257003 (2007).

[26] M. Ovadia, B. Sacépé, and D. Shahar, Phys. Rev. Lett. **102**, 176802 (2009).

[27] T. Levinson, A. Doron, I. Tamir, G. C. Tewari, and D. Shahar, Phys. Rev. B **94**, 174204 (2016).

[28] B. L. Altshuler, V. E. Kravtsov, I. V. Lerner, and I. L. Aleiner, Phys. Rev. Lett. **102**, 176803 (2009).

[29] A. Doron, I. Tamir, S. Mitra, G. Zeltzer, M. Ovadia, and D. Shahar, Phys. Rev. Lett. **116**, 057001 (2016).

[30] See Supplemental Material at http://link.aps.org/supplemental/10.1103/PhysRevB.100.184508 for additional data and description of experimental methods, and see Refs. [41–48].

[31] This is no longer true at $P > 10^{-7}$ W, powers that, in this work, were only applied in the high-bias branch of some IV's. Even in said high biases, the effect of Kapitza resistance that leads to $T_{\rm ph} > T$ has no effect on $T_{\rm el}(P)$ for the range of P's that we have applied, since, even for the highest applied P's, $T_{\rm ph} \ll T_{\rm el}$. A quantitative justification of this statement is located in the Supplemental Material [30].

[32] A. Doron, T. Levinson, F. Gorniaczyk, I. Tamir, and D. Shahar, arXiv:1908.09303.

[33] This analysis hinges on the assumption that all nonlinearities observed in the IV's result solely from electronic heating. This means that $R_{\rm ohm}$ depends on V (or I) only via $T_{\rm el}$, i.e., $R_{\rm ohm} = R_{\rm ohm}(T_{\rm el}(V))$. Using this assumption it is possible to obtain $T_{\rm el}(V)$ by requiring that $R(T_{\rm el}(V)) = V/I(V)$.

[34] The relative error in $Y \equiv IV + \Gamma\Omega T_{\rm ph}^{\beta}$ is $\delta Y/Y \approx [(\partial Y/\partial T_{\rm ph})\delta T_{\rm ph} + (\partial Y/\partial\Gamma)\delta\Gamma + (\partial Y/\partial\beta)\delta\beta]/Y \propto \frac{1}{1+IV/\Gamma\Omega T_{\rm ph}^{\beta}}$, which is highest at low values of IV and is suppressed by a factor of $\frac{\Gamma\Omega T_{\rm ph}^{\beta}}{IV}$ at high bias.

[35] We use the trapping I (or V) as opposed to the escape, which is where the system goes from the low-bias to the high-bias branch, because the escape value often shows stochastic behavior, varying by a significant amount between equivalent measurements. The trapping, on the other hand, is consistently found at a similar value, at the lowest I (or V) in which the high-$T_{\rm el}$ branch is stable.

[36] A. Doron, I. Tamir, T. Levinson, M. Ovadia, B. Sacépé, and D. Shahar, Phys. Rev. Lett. **119**, 247001 (2017).

[37] S. Marnieros, L. Bergé, A. Juillard, and L. Dumoulin, Phys. Rev. Lett. **84**, 2469 (2000).

[38] A. Savin, J. Pekola, M. Prunnila, J. Ahopelto, and P. Kivinen, Phys. Scr. **T114**, 57 (2004).

[39] P. Echternach, M. Thoman, C. Gould, and H. Bozler, Phys. Rev. B **46**, 10339 (1992).

[40] Y. Saito, Y. Kasahara, J. Ye, Y. Iwasa, and T. Nojima, Science **350**, 409 (2015).

[41] Z. Ovadyahu, J. Phys. C: Solid State Phys. **19**, 5187 (1986).

[42] P. L. Kapitza, Phys. Rev. **60**, 354 (1941).

[43] R. C. Johnson and W. Little, Phys. Rev. **130**, 596 (1963).

[44] G. L. Pollack, Rev. Mod. Phys. **41**, 48 (1969).

[45] F. Pobell, *Matter and Methods at Low Temperatures* (Springer, New York, 2007), Vol. 2.

[46] F. C. Wellstood, C. Urbina, and J. Clarke, Phys. Rev. B **49**, 5942 (1994).

[47] O. V. Lounasmaa, *Experimental Principles and Methods Below 1K* (Academic Press, New York, 1974).

[48] E. T. Swartz and R. O. Pohl, Rev. Mod. Phys. **61**, 605 (1989).